Cell Reports
Report

Yeast Endosulfines Control Entry into Quiescence and Chronological Life Span by Inhibiting Protein Phosphatase 2A

Séverine Bontron,[1] Malika Jaquenoud,[1] Stefania Vaga,[2] Nicolas Talarek,[1] Bernd Bodenmiller,[2] Ruedi Aebersold,[2] and Claudio De Virgilio[1,*]
[1]Department of Biology, Division of Biochemistry, University of Fribourg, 1700 Fribourg, Switzerland
[2]Institute of Molecular Systems Biology, ETH Zürich, 8093 Zürich, Switzerland
*Correspondence: claudio.devirgilio@unifr.ch
http://dx.doi.org/10.1016/j.celrep.2012.11.025

SUMMARY

The TORC1 and PKA protein kinases are central elements of signaling networks that regulate eukaryotic cell proliferation in response to growth factors and/or nutrients. In yeast, attenuation of signaling by these kinases following nitrogen and/or carbon limitation activates the protein kinase Rim15, which orchestrates the initiation of a reversible cellular quiescence program to ensure normal chronological life span. The molecular elements linking Rim15 to distal readouts including the expression of Msn2/4- and Gis1-dependent genes involve the endosulfines Igo1/2. Here, we show that Rim15, analogous to the greatwall kinase in *Xenopus*, phosphorylates endosulfines to directly inhibit the Cdc55-protein phosphatase 2A ($PP2A^{Cdc55}$). Inhibition of $PP2A^{Cdc55}$ preserves Gis1 in a phosphorylated state and consequently promotes its recruitment to and activation of transcription from promoters of specific nutrient-regulated genes. These results close a gap in our perception of and delineate a role for $PP2A^{Cdc55}$ in TORC1-/PKA-mediated regulation of quiescence and chronological life span.

INTRODUCTION

Initiation of the quiescence program in eukaryotic cells is a highly coordinated process, which requires proper regulation of growth factor-, hormone-, and nutrient-responsive signal transduction pathways. In yeast, quiescence is primarily induced by limitation for essential nutrients following which cells cease growing, arrest cell division in the G_1 phase of the cell cycle, and acquire a distinct array of physiological, biochemical, and morphological traits. These traits collectively ensure normal chronological life span (CLS) of cells during long periods of starvation and enable them to transit back to the proliferating state upon refeeding.

The decision of yeast cells whether to initiate, or not, the quiescence program relies substantially on the information transmitted by two nutrient signaling pathways. These are the Target Of Rapamycin Complex 1 (TORC1) pathway, which is regulated by the abundance and quality of the available carbon and/or nitrogen source, and the glucose-responsive protein kinase A (PKA) pathway (De Virgilio, 2012; Gray et al., 2004). Attenuation of signaling by these pathways following limitation of the corresponding nutrients activates the protein kinase Rim15, which induces numerous important aspects of the quiescence program (e.g., the expression of specific nutrient-regulated genes and the accumulation of trehalose and glycogen) and critically tailors CLS (Fabrizio et al., 2001; Pedruzzi et al., 2003; Wei et al., 2008). The molecular elements linking Rim15 to distal readouts, however, are only partially characterized. Accordingly, Rim15-dependent phosphorylation of the endosulfines Igo1/2 is essential for mRNAs, which are transcriptionally controlled by the stress response (STRE) and postdiauxic shift (PDS) transcription factors Msn2/4 and Gis1, respectively, to be sheltered from degradation via the 5′-3′ mRNA decay pathway (Cameroni et al., 2004; Luo et al., 2011; Pedruzzi et al., 2000; Talarek et al., 2010). How Rim15 coordinates transcription and posttranscriptional stability of these mRNAs, however, is still mysterious.

Here, we identify the Cdc55-protein phosphatase 2A ($PP2A^{Cdc55}$) as an essential element that links Rim15-Igo1/2-mediated nutrient signaling to downstream effectors, which are key for proper entry into quiescence and CLS. Accordingly, when phosphorylated by Rim15 (on Ser^{64}), Igo1 directly binds to and prevents $PP2A^{Cdc55}$ from dephosphorylating various target proteins including Gis1. In the latter case, conservation of a specific residue (*i.e.* Ser^{425}) in a phosphorylated state promotes recruitment of Gis1 to promoter regions of nutrient-regulated genes. All together, our data suggest a simple model in which Rim15, by activating the $PP2A^{Cdc55}$ inhibitor Igo1, regulates the phosphorylation status and activity of both mRNA decay and transcription factors (such as Gis1) to coordinate entry into quiescence. Interestingly, recent studies in *Xenopus* have shown that the Rim15 orthologous greatwall kinase (Gwl) phosphorylates endosulfines (Ensa and Arpp19) to inhibit the protein phosphatase PP2A-B55δ and consequently promote mitotic progression (Gharbi-Ayachi et al., 2010; Mochida et al., 2010). Based on the remarkable conservation of $PP2A^{Cdc55}$ regulation, which may also extend into downstream effectors, we speculate that Rim15 and Gwl may both be implicated in additional aspects of cell cycle and quiescence/CLS control, respectively.

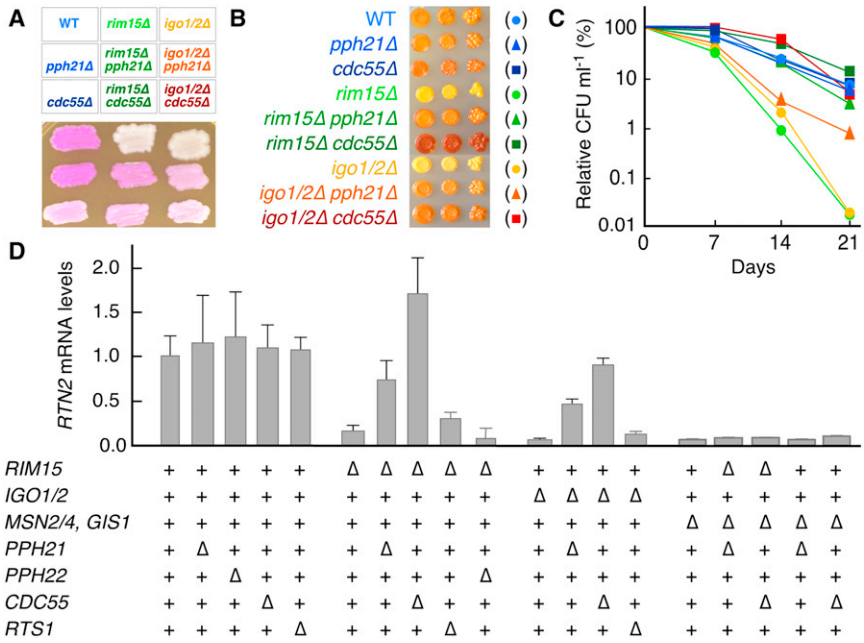

Figure 1. Loss of PP2A^{Cdc55} Suppresses the Defect of *rim15Δ* and *igo1Δ igo2Δ* Cells to Properly Enter Quiescence

(A and B) Analysis of *HSP26p-yEmRFP* expression (A), which confers to cells a purple color, and of glycogen accumulation (visualized by iodine vapor staining) (B), in strains that were patched or spotted on SD-medium-containing plates and grown for 5 days at 30°C. The brown coloration in (B) is proportional to the glycogen content of the cells.

(C) Chronological life span measurements. Survival data (colony forming units [CFUs] ml^{-1}) were expressed as relative values compared to the values at day 0 (which corresponds to day 2 in early stationary phase cultures). Values indicate means of three independent experiments. Symbols and color codes for the strains used are indicated in (B). Notably, in vivo phosphorylation of Ser^{64} in Igo1 requires the presence of Rim15 and is induced in cells entering quiescence and maintained during their subsequent chronological aging (Figure S1A).

(D) qRT-PCR analysis of *RTN2* expression in rapamycin-treated (2.5 hr) cells. The value for the reference sample (rapamycin-treated wild-type cells) was normalized to 1.0. Each bar represents the mean ± SD of three experiments. Genotypes of strains are indicated (+, wild-type gene; Δ, gene deletion[s]). See also Figure S1B.

RESULTS AND DISCUSSION

Loss of PP2A^{Cdc55} Enables *rim15Δ* and *igo1Δ igo2Δ* Cells to Properly Enter Quiescence

To further elucidate the molecular function of Rim15 and its targets Igo1/2, we performed a genome-wide screen for mutations that are able to suppress the defect of *rim15Δ* cells in *HSP26* expression during entry into quiescence (*i.e.* following growth for 5 days on SD plates) as described earlier (Luo et al., 2011). The best hit in this screen turned out to be *pph21Δ*, which was not only able to suppress the defect in *HSP26p-yEmRFP* expression in *rim15Δ*, but also the one in *igo1Δ igo2Δ* double-mutant cells (Figure 1A). Notably, Pph21 and its partially redundant paralog Pph22 function as catalytic protein phosphatase subunits and associate with the scaffold protein Tpd3 and the regulatory subunits Cdc55 or Rts1 to form the heterotrimeric protein complexes PP2A^{Cdc55} or PP2A^{Rts1}, respectively (Jiang, 2006). Since *rts1Δ* did not appear among the positive hits, and since *cdc55Δ* was not scored in our suppressor screen because it was missing in the knockout collection, we deemed it likely that PP2A^{Cdc55}, rather than PP2A^{Rts1}, may play a negative role in *HSP26p-yEmRFP* expression in *rim15Δ* and *igo1Δ igo2Δ* strains. In line with this assumption, we observed that loss of Cdc55 enabled *rim15Δ* as well as *igo1Δ igo2Δ* cells to express *HSP26p-yEmRFP* (Figure 1A). Moreover, we also found that loss of Pph21 or of Cdc55 partially or fully suppressed, respectively, the defects in glycogen accumulation and proper setup of CLS in nutrient-limited *rim15Δ* and *igo1Δ igo2Δ* cells (Figures 1B and 1C).

To corroborate our genetic data, we also quantitatively assessed the expression of *RTN2*, which is strongly induced in a Rim15- and Igo1/2-dependent manner following rapamycin-mediated TORC1 inactivation (Talarek et al., 2010). The data were clear: unlike loss of Rts1 or of Pph22, loss of Pph21 or of Cdc55 partially or fully suppressed, respectively, the *RTN2* expression defect in rapamycin-treated *rim15Δ* and *igo1Δ igo2Δ* cells (Figure 1D; analysis of *SOL4* expression yielded similar results, Figure S1B). Notably, the combined loss of Pph21 and Pph22 rendered cells very sick, but, like loss of Cdc55, also fully suppressed the *RTN2* expression defect in rapamycin-treated *rim15Δ* and *igo1Δ igo2Δ* cells (S.B., unpublished data). Thus, although Pph22 seemingly plays no role on its own in controlling *RTN2* expression (Figure 1D), it appears to provide residual PP2A^{Cdc55} activity in the absence of Pph21. In sum, our genetic data indicate that PP2A^{Cdc55} antagonizes the proper setup of various aspects of the quiescence program both following nutrient limitation and TORC1 inhibition and suggest that Rim15 may negatively regulate PP2A^{Cdc55} via Igo1/2.

Phosphorylation by Rim15 Triggers Igo1 to Bind and Inhibit PP2A^{Cdc55}

Based on both our genetic data and the recent discovery that endosulfines directly inhibit PP2A-B55δ in higher eukaryotes (Gharbi-Ayachi et al., 2010; Mochida et al., 2010), we subsequently performed two-hybrid and coimmunopreciptation (coIP) analyses to verify our assumption that Igo1 may directly interact with PP2A^{Cdc55}. The two-hybrid experiments revealed that Igo1 specifically interacts with Cdc55, but not with Pph21 (Figure 2A). In addition, a Ser^{64} to Ala mutation within Igo1 or loss of Rim15 both abolished the observed Igo1-Cdc55 interaction, indicating that Rim15-mediated phosphorylation of Ser^{64}

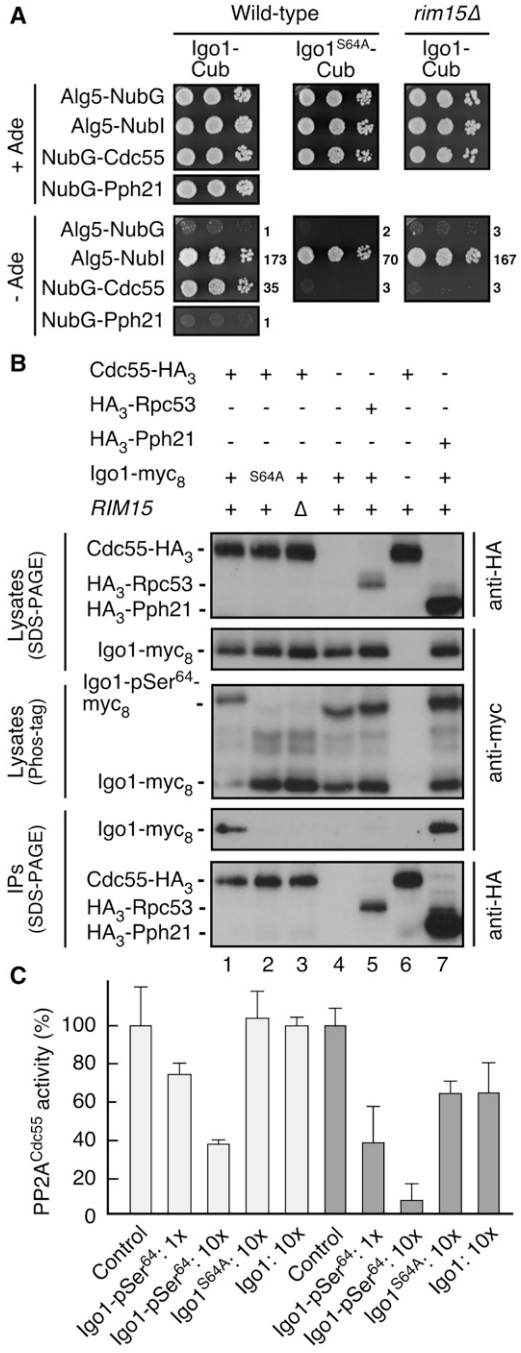

Figure 2. Phosphorylated Igo1 Binds to and Inhibits PP2A^{Cdc55}

(A) Igo1 specifically interacts with Cdc55 in a split-ubiquitin membrane-based yeast two-hybrid assay. The Igo1-Cdc55 interaction is abolished by loss of Rim15 or introduction of a Ser^{64} to Ala mutation in Igo1. Interactions were tested by monitoring growth on plates lacking adenine (−Ade), or β-galactosidase activities (in Miller units; numbers on the right of the panels represent the means of three independent experiments performed with exponentially growing cells), of wild-type and *rim15Δ* cells expressing Igo1-Cub or Igo1^{S64A}-Cub and either Alg5-NubG (negative control), Alg5-NubI (binding any Cub-fusion protein; positive control), NubG-Cdc55, or NubG-Pph21.

(B) Biochemical interaction between PP2A^{Cdc55} and Igo1 phosphorylated at Ser^{64} (Igo1-pSer^{64}). Cdc55-HA$_3$ (lanes 1–3 and 6), untagged Cdc55 (lane 4), HA$_3$-Rpc3 (lane 5), and HA$_3$-Pph21 (lane 7) were immunoprecipitated (using anti-HA affinity matrix; clone 3F10; Roche) from extracts of rapamycin-treated (1.5 hr) cells coexpressing Igo1-myc$_8$ (lanes 1, 3–5, and 7), Igo1^{S64A}-myc$_8$ (lane 2), or untagged Igo1 (lane 6; negative control). Lysates and immunoprecipitates (IPs) were subjected to Phos-tag phosphate-affinity gel electrophoresis (Phos-tag) and/or SDS-PAGE and immunoblots were probed with anti-HA or anti-myc antibodies as indicated. See also Figure S2.

(C) In vitro inhibition of PP2A^{Cdc55} by phosphorylated Igo1 (Igo1-pSer^{64}). Phosphatase activity of purified PP2A^{Cdc55} was analyzed in the presence and absence (control) of recombinant Igo1 or Igo1^{S64A} proteins, which have been subjected to thiophosphorylation by Rim15 prior to use, and expressed as percentage of the control. Nonphosphorylated Igo1 was included as additional control. Phosphatase substrates were either Ser/Thr Phosphatase Substrate I (white bars), which is commonly used to assay PP2A activity, or a synthetic phosphopeptide whose sequence corresponds to the flanking regions of the predicted PP2A^{Cdc55} target residue pSer^{425} within Gis1 (gray bars). In assays with the Gis1-peptide (but not in those with the Ser/Thr Phosphatase Substrate I), nonphosphorylated Igo1, like Igo1^{S64A}, exhibited detectable PP2A^{Cdc55}-inhibitory activity, which was 13-fold lower, however, when compared to the effect of Igo1-pSer^{64}. Each bar represents the mean ± SD of three independent experiments.

within Igo1 is required for it to interact with Cdc55. Our coIP analyses performed on rapamycin-treated cells largely confirmed these results. Accordingly, Igo1-myc$_8$ physically interacted with HA$_3$-tagged Cdc55 and Pph21 (Figure 2B, lanes 1 and 7), but not with HA$_3$-tagged Rpc53, which served as negative control (Figure 2B, lane 5). Moreover, Igo1-myc$_8$ was not able to interact with HA$_3$-tagged Cdc55 if expressed in *rim15Δ* cells or if its Ser^{64} was mutated to Ala (the absence of Igo1 phosphorylated at Ser^{64} [Igo1-pSer^{64}] in these samples was confirmed via Phos-tag phosphate affinity gel electrophoresis; Figure 2B, lanes 2 and 3). Finally, Igo1-myc$_8$ physically interacted with HA$_3$-tagged Cdc55 even in the absence of Pph21, while the interaction between Igo1-myc$_8$ and HA$_3$-tagged Pph21 required the presence of Cdc55 (Figure S2). Igo1 therefore interacts with Pph21 indirectly via Cdc55.

To test whether Igo1 affects the phosphatase activity of PP2A^{Cdc55}, we affinity-purified the heterotrimeric PP2A^{Cdc55} complex from yeast (via HA$_3$-tagged Cdc55) and assayed its activity using a synthetic phosphopeptide (Ser/Thr Phosphatase Substrate I) as substrate. Recombinant Igo1 thiophosphorylated in vitro by Rim15, but not Igo1^{S64A} or unphosphorylated Igo1, strongly inhibited the phosphatase activity of PP2A^{Cdc55} in a concentration-dependent manner (Figure 2C). Thus, analogous to the situation in higher eukaryotes, the yeast endosulfine Igo1 is converted into an inhibitor of PP2A^{Cdc55} by phosphorylation of its Ser^{64} via the greatwall-orthologous Rim15 protein kinase.

Label-free Quantitative Proteomics Screens

Our results so far indicated that inhibition of PP2A^{Cdc55} by the Rim15-Igo1/2 signaling branch is key for cells to gain access to quiescence. To begin to decode the molecular events that critically affect the quiescence program, we tried to identify PP2A^{Cdc55} target proteins by using a label-free quantitative phosphoproteomic approach (Bodenmiller and Aebersold, 2010). To this end, we compared the protein phosphorylation patterns of wild-type, *rim15Δ*, *igo1Δ igo2Δ*, and *pph21Δ* strains prior to and following a 1 hr rapamycin treatment. In total, the

Table 1. Proteins for which Rapamycin-Mediated Increase in Phosphorylation Was Reduced in *rim15Δ* and *igo1Δ igo2Δ* and Enhanced in *pph21Δ* Cells

Protein	Peptide Sequence[a]	Phosphosite
Blm10	S*AT*PTLQDQK	S62, T64
Epo1	MVSANYS*R	S293
Gis1	ISS*PLLSR	S425
Hsp42	DKS*EAPKEEAGETNK	S182
Hxk2	KGS*MADVPKELMQQIENFEK	S15
Pgm3	ASVGVMITAS*HNPK	S158
Sec16	S*NSNVPSLFADFPAPPK	S1576
Smy2	SNT*PLLGGR	T70
Tsl1	SATRS*PSAFNR/IAS*PIQHEHDSGSR	S77/S147
Vts1	SKS*AEPHVNS*SPNLIPVQK	S311, S318
Ymr196w	IGGTHSGLT*PQSSISSDK	T1013
Ypl247c	SS*ISFGSSQR	S12

[a]The phosphorylated serine or threonine residues are marked with an asterisk (S*/T*). For a detailed description of the selection criteria for peptides represented in this list, please see the text. Proteins are sorted by alphabetic order.

eight phosphorylation patterns contained 2,044 distinct phosphopeptides mapping to 830 different proteins (Table S1). In wild-type cells, we found 500 phosphopeptides to be significantly (i.e., >2-fold) upregulated following rapamycin treatment. Among these, the upregulation of 162 and 98 phosphopeptides was diminished more than 2-fold in *rim15Δ* and *igo1Δ igo2Δ* cells, respectively. To identify the most likely PP2A^{Cdc55} targets, we then selected, among the 64 phosphopeptides that showed diminished upregulation in both rapamycin-treated *rim15Δ* and *igo1Δ igo2Δ* mutant cells, the ones that were at least 1.9-fold upregulated in *pph21Δ* cells under the same conditions. Intriguingly, among the remaining 13 phosphopeptides (Table 1), two mapped to proteins, i.e., Vts1 and Gis1, which have previously been implicated in regulating gene expression of nutrient-controlled genes. Vts1 is a member of the Smaug family of proteins, which directly binds target mRNAs and regulates their stability by interfering with the 5′-3′ mRNA decay pathway (Rendl et al., 2008), and Gis1 is a transcription factor, which plays a key role in proper setup of quiescence and CLS downstream of Rim15 (Pedruzzi et al., 2000). Here, we focus our analyses on Gis1, which—together with Msn2/4 that substitute to some extent Gis1 function in *gis1Δ* cells (S.B., unpublished data)—is required for rapamycin-induced *RTN2* and *SOL4* expression in wild-type, *rim15Δ cdc55Δ*, or *rim15Δ pph21Δ* cells (Figures 1D and S1B).

Gis1 Is a PP2A^{Cdc55} Target

To validate the results of our phosphoproteome studies, we examined the migration pattern of Gis1-HA$_3$ by phosphate affinity gel electrophoresis in different yeast strains. When analyzed in extracts of exponentially growing wild-type, *rim15Δ* and *igo1Δ igo2Δ* cells, Gis1-HA$_3$ migrated in at least three distinct bands. Following rapamycin treatment, these bands collapsed into one slow-migrating form in wild-type, but not in *rim15Δ* and *igo1Δ igo2Δ* cells (Figure 3A). The latter defect in *rim15Δ* and *igo1Δ igo2Δ* cells could be cured by loss of Pph21 or Cdc55. Interestingly, in exponentially growing *cdc55Δ* cells, Gis1-HA$_3$ was detectable only in its slow-migrating form independently of the presence or absence of Rim15 or Igo1/2 (Figure 3A). This was not the case in exponentially growing *pph21Δ* cells, which likely exhibit residual PP2A^{Cdc55} activity due to the presence of Pph22. Thus, in exponentially growing cells, PP2A^{Cdc55} specifically targets presumably two (or more) phosphorylated residues in Gis1, which account for the protein bands observed in wild-type samples. Together, these results indicate that in rapamycin-treated cells, Rim15-activated Igo1/2 specifically antagonize PP2A^{Cdc55}-mediated dephosphorylation of Gis1. In line with this model we further found that PP2A^{Cdc55} was able to dephosphorylate in vitro a synthetic phosphopeptide corresponding in sequence to the flanking regions of the predicted Pph21 target residue pSer^{425} within Gis1 (Table 1), and that Igo1-pSer^{64} strongly inhibited this activity in a concentration-dependent manner (Figure 2C). Moreover, in coIP experiments using extracts of exponentially growing cells, Gis1-myc$_{13}$ bound Cdc55-HA$_3$ or HA$_3$-Pph21, but not HA$_3$-Nap1 (control), whereas mutation of Ser^{425} to Ala in Gis1 or treatment of cells with rapamycin strongly reduced the observed interactions (Figure 3B).

Albeit Ser^{425} is unlikely to be the only PP2A^{Cdc55}-regulated phosphoresidue in Gis1, we addressed the possibility that phosphorylation of Gis1-Ser^{425} may be functionally relevant in vivo. To this end, we used a *PDS-lacZ* reporter, which depends entirely on the presence of Gis1 for its expression following glucose-limitation (Pedruzzi et al., 2000) (Figure 3C). In these assays, Gis1^{S425A}-overexpressing cells exhibited significantly reduced *PDS-lacZ* expression when compared to Gis1-overexpressing control cells (Figure 3C). Similarly, plasmid-encoded, overexpressed Gis1^{S425A} was less efficient than Gis1 in restoring to *msn2/4Δ gis1Δ* triple mutants their ability to express *RTN2* following rapamycin treatment (Figure 3D). Loss of Pph21 or of Cdc55 did not diminish the relative *RTN2* expression defect in Gis1^{S425A}- versus Gis1-overexpressing cells, as expected, but it generally resulted in higher basal levels of rapamycin-induced *RTN2* expression. Thus, in addition to corroborating our assumption that Ser^{425} is a functionally relevant PP2A^{Cdc55} target residue within Gis1, these data indicate that PP2A^{Cdc55} regulates Gis1 function also via a Ser^{425}-independent mechanism. To further address the mechanism by which the Ser^{425} residue controls Gis1 function, we also studied (via Chromatin IP [ChIP] assays) whether Ser^{425} may be critical for Gis1 recruitment to the *RTN2* promoter. In line with our *RTN2* expression data (Figure 3D), we observed that binding of Gis1 to the *RTN2* promoter increased following rapamycin treatment and that this increase was significantly reduced when Ser^{425} within Gis1 was mutated to Ala (Figure 3E). Moreover, loss of Rim15 or of Igo1/2 also diminished the rapamycin-induced recruitment of Gis1 to the *RTN2* promoter, which could be largely prevented by introduction of a *cdc55Δ* mutation in these strains. Since loss of Rim15 or Igo1/2 affects *RTN2* promoter binding of Gis1 more strongly than the Ser^{425} to Ala mutation in Gis1 (Figure 3E), these data also indicate that PP2A^{Cdc55} regulates Gis1 promoter recruitment in part independently of Ser^{425}.

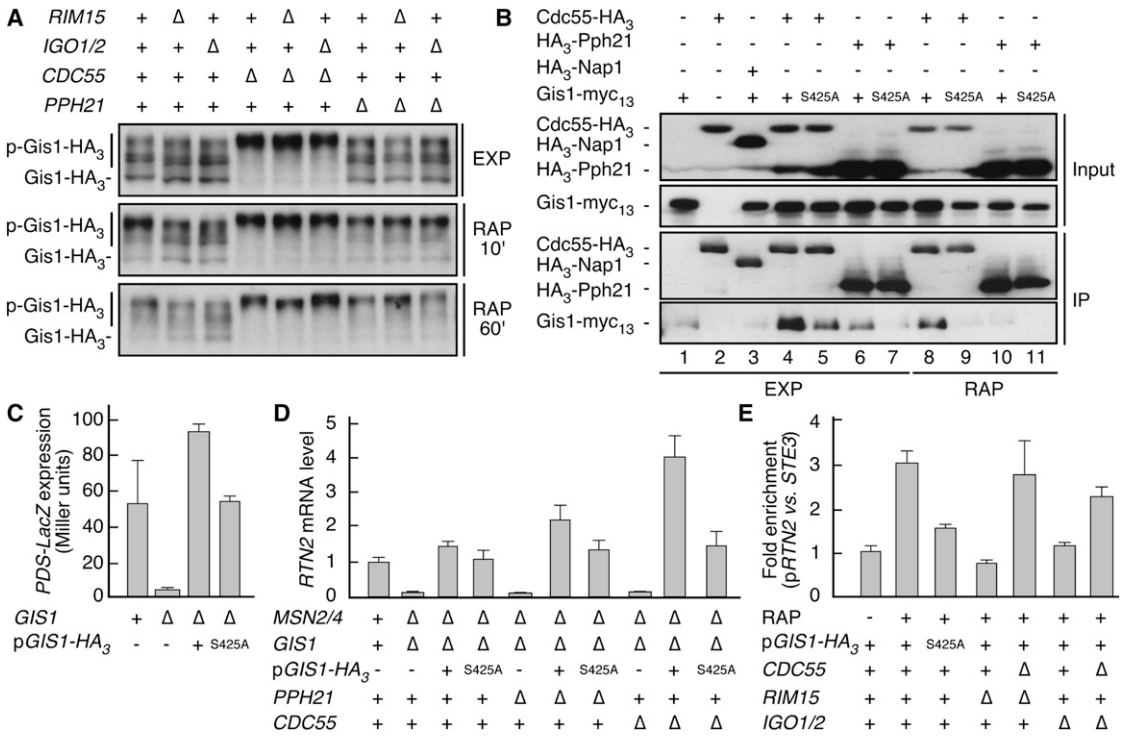

Figure 3. PP2A^{Cdc55} Regulates Phosphorylation and Consequently Promoter Recruitment of Gis1

(A) Phos-tag phosphate-affinity gel electrophoresis analysis of the phosphorylation pattern of Gis1-HA$_3$ in exponentially growing (EXP) and rapamycin-treated (RAP; 10 or 60 min) wild-type and indicated mutant strains (+, wild-type gene; Δ, gene deletion[s]). p-Gis1-HA$_3$ denotes hyperphosphorylated forms of Gis1-HA$_3$.

(B) Biochemical interaction between PP2A^{Cdc55} and Gis1. Cdc55-HA$_3$ (lanes 2, 4, 5, 8, and 9), untagged Cdc55 (lane 1), HA$_3$-Nap1 (lane 3; unrelated control protein), and HA$_3$-Pph21 (lanes 6, 7, 10, and 11) were immunoprecipitated (as in Figure 2B) from extracts of exponentially growing (EXP) or rapamycin-treated (RAP; 90 min) cells coexpressing, or not (lane 2), Gis1-myc$_{13}$ (lanes 1, 3, 4, 6, 8, and 10) or Gis1^{S425A}-myc$_{13}$ (lanes 5, 7, 9, and 11).

(C) *PDS-LacZ* expression (in Miller units) in glucose-limited (i.e.. postdiauxic) wild-type (*GIS1*; +) or *gis1Δ* (*GIS1*; Δ) cells carrying an empty vector (−), or a plasmid driving overexpression of wild-type Gis1-HA$_3$ (p*GIS1-HA$_3$*; +) or Gis1^{S425A}-HA$_3$ (p*GIS1^{S425A}-HA$_3$*; S425A).

(D) qRT-PCR analysis of *RTN2* expression following rapamycin treatment (2.5 hr) in wild-type and indicated mutant cells carrying an empty vector (−), or a plasmid driving overexpression (from the *ADH1* promoter) of wild-type Gis1-HA$_3$ (p*GIS1-HA$_3$*; +) or Gis1^{S425A}-HA$_3$ (p*GIS1^{S425A}-HA$_3$*; S425A). The value for the reference sample (rapamycin-treated wild-type cells) was normalized to 1.0. For details, see legend of Figure 1D. Protein levels of Gis1-HA$_3$ and Gis1^{S425A}-HA$_3$ were verified by immunoblotting (Figure S3).

(E) ChIP analysis of Gis1-HA$_3$ and Gis1^{S425A}-HA$_3$ recruitment to the *RTN2* promoter (p*RTN2*; normalized with respect to the unrelated genomic region of *STE3*). Gis1-HA$_3$ (p*GIS1-HA$_3$*; +) and Gis1^{S425A}-HA$_3$ (p*GIS1^{S425A}-HA$_3$*; S425A) were overexpressed from plasmids. ChIPs were performed in samples drawn either from exponentially growing (RAP; −) or rapamycin-treated (RAP; +; 2.5 hr) wild-type or indicated mutant strains. The value for the reference sample (exponentially growing wild-type cells overexpressing Gis1-HA$_3$) was normalized to 1.0. In Figures 2C–2E, each bar represents the mean ± SD of three experiments.

In conclusion, all of our data are consistent with a model in which Rim15 controls transcription of a specific set of nutrient-controlled genes by regulating the phosphorylation status, and hence promoter recruitment of Gis1 indirectly via the Igo1-PP2A^{Cdc55} effector branch. Extending our previous conclusions (Talarek et al., 2010), our current study therefore suggests that Rim15 coordinates both aspects of gene expression, i.e., transcriptional activation and protection of the respective transcripts from 5′-3′ mRNA decay pathway-mediated degradation, by activating Igo1/2 and consequent inhibition of PP2A^{Cdc55}. Future studies should therefore address the possibility that Rim15 itself may be recruited to specific promoter regions to coordinate local activation of transcription and ensure cotranscriptional loading of activated Igo1 onto newly forming messenger ribonucleoprotein (mRNP) complexes, which may be key to control the phosphorylation status and activity of 5′-3′ mRNA decay pathway proteins within these complexes. Notably, in this context, Vts1 (Table 1) binds an RNA motif, which occurs specifically in a set of genes that are induced in cells entering quiescence (Riordan et al., 2011). In addition, a large fraction of the genes whose expression is most strongly affected by loss of Vts1 (including *RTN2* and *SOL4*) appears to also be regulated by Rim15-Igo1/2 (Oberstrass et al., 2006; Talarek et al., 2010). It will therefore be interesting to also explore a mechanistically different model in which temporally coordinated, but parallel regulation by the Igo1/2-PP2A^{Cdc55} module of both Gis1 and Vts1 may allow cells to coordinate transcription and posttranscriptional mRNA stability of Gis1-dependent genes containing a Vts1 RNA-binding motif.

Together with previous studies (for a recent review, see Longo et al., 2012), our current data show that the Rim15-Igo1/2-PP2A^{Cdc55} module represents an element of a TORC1-controlled effector branch, which plays a major role in shaping both the cellular quiescence program and CLS in yeast. Given the universal role of TORC1 in CLS regulation (Fontana et al., 2010), as well as the remarkable conservation of the Rim15-Igo1/2-PP2A^{Cdc55} module, it will be interesting to examine whether the Gwl-Ensa/Arpp19-PP2A-B55δ signaling branch may also regulate CLS in higher eukaryotes via similar mechanisms as described here in yeast. Conversely, given the important role of Gwl-Ensa/Arpp19-PP2A-B55δ in regulating mitosis in higher eukaryotes (Mochida and Hunt, 2012), future studies should also address the possibility that Rim15-Igo1/2-PP2A^{Cdc55} may contribute to the control of cell cycle events in yeast.

EXPERIMENTAL PROCEDURES

Strains, Growth Conditions, and Plasmids

S. cerevisiae strains (Table S2) were grown at 30°C in standard rich medium (YPD) with 2% glucose or in synthetic defined (SD) medium (0.17% yeast nitrogen base, 0.5% ammonium sulfate, and 2% glucose) complemented with the appropriate nutrients for plasmid maintenance. Rapamycin was used at a concentration of 200 ng ml^{-1}. The plasmids used in this study are listed in Table S3.

Quantitative Real-Time PCR

Total RNA was extracted using the hot acidic phenol method. DNA was removed with the DNA-free Kit (Applied Biosystems) and first-strand cDNA was synthesized with the PrimeScript RT Reagent Kit (TaKaRa). Quantitative RT-PCR (qRT-PCR) was performed on a Rotor-Gene 6000 machine (Corbett Life Science), with the 5 × EvaGreen QPCR Mix II (no Rox; Bio&SELL). Oligonucleotides used for qRT-PCR are listed in Table S4. *RTN2* and *SOL4* mRNA levels were normalized with respect to *TBP1* mRNA.

Chromatin Immunoprecipitation

Chromatin immunoprecipitation (ChIP) was performed mainly as published (Aparicio et al., 2005) using cells that were fixed for 15 min at 30°C with 1% formaldehyde. The lysates were sonicated for six cycles (15 s on, 1 s off) with a Misonix 3000 sonicator. Gis1-HA$_3$ or Gis1^{S425A}-HA$_3$ were IPed overnight at 4°C using anti-HA antibodies (ab9110; abcam) and protein-G agarose and DNA was analyzed by qPCR (see Table S4 for oligonucleotides). Signals for the *RTN2* promoter were normalized with respect to the unrelated genomic region of *STE3*.

Phosphatase Assays

The PP2A^{Cdc55} complex was isolated from exponentially growing *cdc55Δ* cells carrying the p416-*ADH1p-CDC55-HA$_3$* plasmid. PP2A^{Cdc55} was IPed from 140 mg total extract in lysis buffer (50 mM HEPES-KOH [pH 7.6], 1 M KCl, 1 mM $MgCl_2$, 1 mM EGTA, 5% glycerol, 0.45% Tween-20, 2 mM PMSF, and one tablet of Complete Protease Inhibitor Cocktail [Roche Diagnostics GmbH] per 50 ml) using anti-HA antibodies (12CA5) and protein-G agarose. The integrity of the PP2A^{Cdc55} complex was assessed via western blot analysis using anti-HA, anti-Tpd3, and anti-Pph21 antibodies. Igo1-His$_6$ and Igo1^{S64A}-His$_6$ were isolated from bacteria with Ni-NTA resin (QIAGEN) and phosphorylated when indicated by GST-Rim15-HA$_3$ using 1 mM adenosine 5′-[γ-thio] triphosphate (Reinders et al., 1998). The in vitro phosphatase assay (60 min at 30°C) was performed in 50 μl PP2A buffer (20 mM Tris [pH 7.5], 5 mM $MgCl_2$, 0.02% β-mercaptoethanol, and 1 mM EGTA) with 1/60th of the PP2A^{Cdc55} purification, 100 μM Ser/Thr Phosphatase Substrate I (DLDVPIPGRFDRRVpSVAAE; R&D Systems) or 200 μM Gis1-pSer^{425} substrate (TISRISpSPLLSRMMDLSNIVEPTLDDP; Thermo Scientific), and either 0 (control), 25 ng (1×), or 250 ng (10×) Igo1 (or Igo1^{S64A}) that was, or was not, subjected to in vitro phosphorylation by Rim15 prior to use. To assess PP2A activity, the released phosphate was measured using BIOMOL GREEN (ENZO Life Sciences).

CoIP and Phos-tag Phosphate-Affinity Gel Electrophoresis

Cells were fixed (Figures 2B and S2), or not (Figure 3B), for 20 min with 1% formaldehyde. After quenching with 0.3 M glycine, whole cell extracts were prepared and incubated with an anti-HA affinity matrix (clone 3F10; Roche). Phosphorylation of Gis1-HA$_3$ and Igo1-myc$_8$ was assessed by loading trichloroacetic acid (TCA) whole-cell extracts or lysates on 7.5% SDS-PAGE gels containing 25 μM Phos-tag (Wako).

Phosphoproteomics Sample Preparation and Analysis by Label-free Quantification

All the budding yeast samples for the phosphoproteomics analysis were processed as described (Bodenmiller and Aebersold, 2010). Briefly, cultures (all in triplicates) were incubated on ice for 10 min in the presence of 6.25% ice cold TCA before pelleting. For each replicate, 3 mg proteins were digested by trypsin (1:125 w/w) and cleaned by reverse-phase chromatography. Phosphopeptide isolation was performed by titanium dioxide resin (1.25 mg resin for each sample). Isolated phosphopeptides were analyzed by a LTQ FT Ultra mass spectrometer (Thermo Scientific, Germany), interfaced with a nanoelectrospray ion source. Chromatographic separation of peptides was performed on a Proxeon Easy-nLC II system (Odense, Denmark) using a 10.5 cm × 75 μm column packed with 3 μm Magic C18 material. Peptides were separated at a flow rate of 300 nl min^{-1} with a gradient increasing from 5 to 40% acetonitrile. The five most intense ions detected in each MS1 scan were selected for fragmentation. The mass spectrometry data were searched against an SGD decoy database for yeast proteins using Sequest (Lundgren et al., 2009). OpenMS version 1.7 (Sturm et al., 2008) was used both to detect MS1 features and to align them between the different experimental conditions. By using a decoy database (Käll et al., 2008), a Peptide Prophet's probability threshold was computed in order to achieve a false discovery rate below 1%, and was used to filter OpenMS results. Phosphopeptides features with identical sequence and phosphorylation state, but different charge states, were merged together.

SUPPLEMENTAL INFORMATION

Supplemental Information includes three figures and four tables and can be found with this article online at http://dx.doi.org/10.1016/j.celrep.2012.11.025.

LICENSING INFORMATION

ACKNOWLEDGMENTS

We thank Bénédicte Zufferey and Patricia Matthey for technical assistance, Egon Ogris and David Pallas for antibodies, and Marie-Pierre Péli-Gulli for critical comments on the manuscript. This research was supported by the Canton of Fribourg and the Swiss National Science Foundation (C.D.V.).

Received: September 12, 2012
Revised: November 12, 2012
Accepted: November 28, 2012
Published: December 27, 2012

REFERENCES

Aparicio, O., Geisberg, J.V., Sekinger, E., Yang, A., Moqtaderi, Z., and Struhl, K. (2005). Chromatin immunoprecipitation for determining the association of proteins with specific genomic sequences in vivo. Curr. Protoc. Mol. Biol. *Chapter 21*, *Unit 21.23*.

Bodenmiller, B., and Aebersold, R. (2010). Quantitative analysis of protein phosphorylation on a system-wide scale by mass spectrometry-based proteomics. Methods Enzymol. *470*, 317–334.

Cameroni, E., Hulo, N., Roosen, J., Winderickx, J., and De Virgilio, C. (2004). The novel yeast PAS kinase Rim 15 orchestrates G_0-associated antioxidant defense mechanisms. Cell Cycle *3*, 462–468.

De Virgilio, C. (2012). The essence of yeast quiescence. FEMS Microbiol. Rev. *36*, 306–339.

Fabrizio, P., Pozza, F., Pletcher, S.D., Gendron, C.M., and Longo, V.D. (2001). Regulation of longevity and stress resistance by Sch9 in yeast. Science *292*, 288–290.

Fontana, L., Partridge, L., and Longo, V.D. (2010). Extending healthy life span—from yeast to humans. Science *328*, 321–326.

Gharbi-Ayachi, A., Labbé, J.C., Burgess, A., Vigneron, S., Strub, J.M., Brioudes, E., Van-Dorsselaer, A., Castro, A., and Lorca, T. (2010). The substrate of Greatwall kinase, Arpp19, controls mitosis by inhibiting protein phosphatase 2A. Science *330*, 1673–1677.

Gray, J.V., Petsko, G.A., Johnston, G.C., Ringe, D., Singer, R.A., and Werner-Washburne, M. (2004). "Sleeping beauty": quiescence in *Saccharomyces cerevisiae*. Microbiol. Mol. Biol. Rev. *68*, 187–206.

Jiang, Y. (2006). Regulation of the cell cycle by protein phosphatase 2A in *Saccharomyces cerevisiae*. Microbiol. Mol. Biol. Rev. *70*, 440–449.

Käll, L., Storey, J.D., MacCoss, M.J., and Noble, W.S. (2008). Assigning significance to peptides identified by tandem mass spectrometry using decoy databases. J. Proteome Res. *7*, 29–34.

Longo, V.D., Shadel, G.S., Kaeberlein, M., and Kennedy, B. (2012). Replicative and chronological aging in *Saccharomyces cerevisiae*. Cell Metab. *16*, 18–31.

Lundgren, D.H., Martinez, H., Wright, M.E., and Han, D.K. (2009). Protein identification using Sorcerer 2 and SEQUEST. Curr. Protoc. Bioinformatics *Chapter 13*, *Unit 13.13*.

Luo, X., Talarek, N., and De Virgilio, C. (2011). Initiation of the yeast G_0 program requires Igo1 and Igo2, which antagonize activation of decapping of specific nutrient-regulated mRNAs. RNA Biol. *8*, 14–17.

Mochida, S., and Hunt, T. (2012). Protein phosphatases and their regulation in the control of mitosis. EMBO Rep. *13*, 197–203.

Mochida, S., Maslen, S.L., Skehel, M., and Hunt, T. (2010). Greatwall phosphorylates an inhibitor of protein phosphatase 2A that is essential for mitosis. Science *330*, 1670–1673.

Oberstrass, F.C., Lee, A., Stefl, R., Janis, M., Chanfreau, G., and Allain, F.H. (2006). Shape-specific recognition in the structure of the Vts1p SAM domain with RNA. Nat. Struct. Mol. Biol. *13*, 160–167.

Pedruzzi, I., Bürckert, N., Egger, P., and De Virgilio, C. (2000). *Saccharomyces cerevisiae* Ras/cAMP pathway controls post-diauxic shift element-dependent transcription through the zinc finger protein Gis1. EMBO J. *19*, 2569–2579.

Pedruzzi, I., Dubouloz, F., Cameroni, E., Wanke, V., Roosen, J., Winderickx, J., and De Virgilio, C. (2003). TOR and PKA signaling pathways converge on the protein kinase Rim15 to control entry into G_0. Mol. Cell *12*, 1607–1613.

Reinders, A., Bürckert, N., Boller, T., Wiemken, A., and De Virgilio, C. (1998). *Saccharomyces cerevisiae* cAMP-dependent protein kinase controls entry into stationary phase through the Rim15p protein kinase. Genes Dev. *12*, 2943–2955.

Rendl, L.M., Bieman, M.A., and Smibert, C.A. (2008). *S. cerevisiae* Vts1p induces deadenylation-dependent transcript degradation and interacts with the Ccr4p-Pop2p-Not deadenylase complex. RNA *14*, 1328–1336.

Riordan, D.P., Herschlag, D., and Brown, P.O. (2011). Identification of RNA recognition elements in the *Saccharomyces cerevisiae* transcriptome. Nucleic Acids Res. *39*, 1501–1509.

Sturm, M., Bertsch, A., Gröpl, C., Hildebrandt, A., Hussong, R., Lange, E., Pfeifer, N., Schulz-Trieglaff, O., Zerck, A., Reinert, K., and Kohlbacher, O. (2008). OpenMS - an open-source software framework for mass spectrometry. BMC Bioinformatics *9*, 163.

Talarek, N., Cameroni, E., Jaquenoud, M., Luo, X., Bontron, S., Lippman, S., Devgan, G., Snyder, M., Broach, J.R., and De Virgilio, C. (2010). Initiation of the TORC1-regulated G_0 program requires Igo1/2, which license specific mRNAs to evade degradation via the 5′-3′ mRNA decay pathway. Mol. Cell *38*, 345–355.

Wei, M., Fabrizio, P., Hu, J., Ge, H., Cheng, C., Li, L., and Longo, V.D. (2008). Life span extension by calorie restriction depends on Rim15 and transcription factors downstream of Ras/PKA, Tor, and Sch9. PLoS Genet. *4*, e13.